Author Manuscript

Author Manuscript

Author Manuscript

Author Manuscript

HHS Public Access

Author manuscript

Chemistry. Author manuscript; available in PMC 2016 February 16.

Published in final edited form as:

Chemistry. 2015 February 16; 21(8): 3156–3166. doi:10.1002/chem.201405253.

NMR Hyperpolarization Techniques for Biomedicine

Dr. Panayiotis Nikolaou[a], **Prof. Boyd M. Goodson**[b], and **Prof. Eduard Y. Chekmenev**[a]

Eduard Y. Chekmenev: eduard.chekmenev@vanderbilt.edu

[a]Institute of Imaging Science (VUIIS), Department of Radiology, Department of Biomedical Engineering, Department of Physics and Astronomy and Department of Biochemistry, Vanderbilt-Ingram Cancer Center (VICC), Vanderbilt University, 1161 21st Ave South AA-1107, Nashville, Tennessee, 37232-2310 (United States)

[b]Department of Chemistry and Biochemistry, Southern Illinois University, Carbondale, Illinois, 62901 (United States)

Abstract

Recent developments in NMR hyperpolarization have enabled a wide array of new *in vivo* molecular imaging modalities—ranging from functional imaging of the lungs to metabolic imaging of cancer. This Concept article explores selected advances in methods for the preparation and use of hyperpolarized contrast agents, many of which are already at or near the phase of their clinical validation in patients.

Keywords

hyperpolarization; Dynamic Nuclear Polarization; parahydrogen; molecular imaging; Spin Exchange Optical Pumping

Introduction

The first known attempts to split spectroscopic lines of particles using an applied magnetic field date back to Michael Faraday in 1862.[1] However, the effect was not realized until Pieter Zeeman's discovery in 1897 of field-induced broadening of sodium spectra lines.[1] The Zeeman effect of energy-level splitting of *nuclear* spin states in a static magnetic field is fundamental for Nuclear Magnetic Resonance (NMR). For spin ½ nuclei, there are two such energy levels separated by $\Delta E = -\gamma\hbar B_0$, where γ is the gyromagnetic ratio for the nuclear spin of a given isotope, $\hbar = h/2\pi$, h is Planck's constant, and B_0 is the applied static magnetic field strength. Unlike in optical and other spectroscopic methods, wherein the entire ensemble (or large fractions of the ensemble) give rise to signal formation—conventional NMR represents a special case: here, the energy level spacing is much less than the ambient thermal energy (kT), and thus the different energy levels are nearly equally populated. Unfortunately, it is this minute difference among the populations of nuclear spin Zeeman energy levels—usually referred to as nuclear spin polarization (P) or the degree of nuclear spin alignment with the applied magnetic field—that in fact contributes to the

Correspondence to: Eduard Y. Chekmenev, eduard.chekmenev@vanderbilt.edu.

Author Manuscript Author Manuscript Author Manuscript Author Manuscript

detectable NMR signal. As governed by the Boltzmann distribution, it can be shown that $P \approx \Delta E/2kT$ or $P \approx \gamma\hbar B_0/2kT$ (using the above equation) under thermal equilibrium conditions. Biomedical or *in vivo* applications of NMR imply temperatures approximately 300 K, and even when high magnetic fields (up to tens of Tesla) are applied, nuclear spin polarization P remains relatively low (10^{-6}-10^{-4}) for biomedically relevant nuclei such as ^{1}H, ^{13}C, ^{15}N, ^{129}Xe, and others. This low value of P directly reflects the fraction of the nuclear spin ensemble contributing to the NMR signal (the rest are quite literally "radio-silent")--explaining why NMR and MRI are frequently called low-sensitivity techniques in comparison to other spectroscopic and imaging modalities.

However, in some cases P can be artificially—albeit transiently—increased well above its low thermal equilibrium level. This possibility was demonstrated at the dawn of NMR by Carver and Slichter in 1953, when they increased P of ^{7}Li nuclei through polarization transfer from free electrons.[2] This significant (usually orders-of-magnitude) increase in nuclear spin polarization above the thermal-equilibrium level was later called *hyperpolarization*. The increase in polarization may be quantified by the *polarization enhancement* factor ε—defined as the ratio of the nuclear spin polarization in HP state and that obtained at thermal equilibrium. Because the NMR signal is directly proportional to the nuclear spin polarization, the realized polarization enhancement manifests in the corresponding NMR signal and corresponding gains in detection sensitivity, which can be ~4–5 orders of magnitude at high field and even greater at lower fields.[3] Despite these significant gains in sensitivity achieved through hyperpolarization, the energy of RF-quanta remains low, and the overall sensitivity remains relatively low as compared, *e.g.*, to optical methods.

In the more than 60 years since the first hyperpolarization demonstration, a number of hyperpolarization techniques have been developed and applied to pure elements, chemical compounds and complex mixtures with potential or realized biomedical relevance.[4] These HP compounds can be administered to patients via intravenous (IV) injection or inhalation to trace metabolism and function in living organisms, as well as for other biomedical applications. Because the produced HP substances (also referred to as HP contrast agents) generally cannot be re-hyperpolarized after their administration, the hard-won HP state will exponentially decay back to equilibrium. This decay ostensibly poses a fundamental limit on the time scale of biochemical processes that can be probed by HP contrast agents, and requires HP lifetimes that are sufficiently long (≥tens of seconds) for agent manipulation after its production, administration (*e.g.* inhalation or injection), *in vivo* delivery, and observation of the metabolic/functional event. The unrecoverable nature of the HP state additionally requires highly specialized MR pulse sequences that are tailored to extract as much information as possible from the HP contrast agents. However, such efficient sequences—combined with the bright HP-endowed signal—can enable high-quality clinical 3D images of HP contrast agents to be obtained in as little as a few seconds.[5] Moreover, because the HP nuclear state is no longer endowed by the static magnetic field of the detecting MR magnet, high-field MRI scanners are no longer mandatory, and lower-cost, less-confining, *low*-field 3D MRI can be used instead[6]—with detection sensitivity potentially approaching or even surpassing that of high-field MRI.[7]

Author Manuscript Author Manuscript Author Manuscript Author Manuscript

While numerous hyperpolarization methods and strategies have been developed, this Concept article describes four methods of hyperpolarization: dissolution Dynamic Nuclear Polarization (d-DNP),[8] Spin Exchange Optical Pumping (SEOP),[9] Parahydrogen Induced Polarization (PHIP),[10] and Signal Amplification by Reversible Exchange (SABRE).[11] These HP methods arguably have the greatest relevance to biomedicine, given that they have each either already been tested in patients or animals models of human diseases—or have great potential and will likely be tested *in vivo* soon. The fundamental MR detection concepts of HP contrast are also discussed from the perspective of biomedical applications. Finally, existing and potential biomedical applications of already-available and emerging HP contrast agents are discussed. While validated and emerging concepts are discussed here, the reader should additionally benefit from more comprehensive reviews on selected topics.[4, 9, 12]

Long-Lived Spin States

Values for the *in vivo* spin-lattice relaxation time constant (T_1) for protons of water (~1.5 s[13]) and other biologically relevant and abundant molecules are usually too short to be useful for HP biomedical applications. However, T_1 values of low-γ spin-½ nuclei (e.g. ^{13}C, ^{15}N, ^{129}Xe, ^{29}Si, etc.[14]) can significantly exceed 1 minute. From a molecular perspective, these long times typically represent spin sites isolated from protons and paramagnetic O_2 to reduce the relaxation contribution via dipolar mechanisms. Examples include ^{13}C-carboxyl sites,[15] noble gases like ^{129}Xe[5b] and ^{3}He, $^{15}N_2O$,[16] ^{29}Si in silicon nanoparticles,[14] and quaternary and tertiary ^{15}N-amines.[17] ^{13}C-carboxyl sites are of particular interest because of their wide distribution in major metabolic pathways such as anaerobic glycolysis, tricarboxylic acid cycle (TCA) cycle, glutaminolysis, and many others.[4] Notably, the natural abundances of many biologically relevant isotopes such as ^{13}C and ^{15}N (1.1% and 0.36% respectively) are low—representing both an advantage (low background signal) and a challenge (a requirement for isotopic enrichment to boost the detection sensitivity). An alternative approach for increasing the effective lifetime of HP agents introduced relatively recently involves the use long-lived *singlet* states. In this approach, the high nuclear spin order of the HP state—which otherwise would be subject to the usual relaxation mechanisms quantified by T_1—is instead "encoded" and stored within a coupled spin pair's *singlet* state of the form: $|\mathbf{S}_0\rangle \propto (|\alpha\beta\rangle - |\beta\alpha\rangle)$; parahydrogen, discussed in greater detail below, contains perhaps the simplest example of a nuclear spin system in a singlet state. The decay of spin order "trapped" within a singlet state is governed by the singlet-triplet interconversion time constant (T_S), which in some circumstances can surpass T_1 values by orders of magnitude.[16, 18] Regardless of the approaches chosen for hyperpolarization preparation and storage, their applicability is often limited to a narrow range of useful HP targets—particularly when one has a given potential application in mind. This fact highlights the challenges and opportunities for innovative concepts of this rapidly emerging field of molecular imaging, where fundamental chemistry, NMR spectroscopy, and spin physics have direct and practical implications for biomedicine.

Author Manuscript Author Manuscript Author Manuscript Author Manuscript

Dissolution Dynamic Nuclear Polarization (d-DNP)

d-DNP[8] relies on unpaired electrons as the source of large spin polarization in a manner similar to pioneering experiments by Carver and Slichter,[2] because $\gamma(e) \approx 660\gamma(^1H)$. Indeed, when electrons are subjected to sufficiently low temperatures in a static magnetic field of several Tesla, order-unity electronic polarization can be attained.

To enable the d-DNP process, a compound containing a stable free radical (e.g. the trityl radical(tris{8-carboxyl-2,2,6,6-tetra[2-(1-hydroxyethyl)]-benzo(1,2-d:4,5-d')bis(1,3)dithiole-4-yl}methyl sodium salt[8]) is first mixed with a biomolecule of interest (e.g. 1-^{13}C-pyruvic acid) in a solution to form a glass matrix at low temperature inside high-field magnet, Figure 1a. This glass matrix is then irradiated with a high-power microwave source at the electron resonance frequency to transfer electron spin polarization to ^{13}C nuclear spins in the solid state, Figure 2b. The exponential build-up of ^{13}C hyperpolarization was rather slow (~4,900 s for 1-^{13}C-pyruvic acid) in the original DNP hyperpolarizer by Ardenkjaer-Larsen and co-workers.[8] However, the ^{13}C hyperpolarization build-up time can be significantly minimized if the electron polarization is first transferred to the proton spin bath of the matrix, and then from ^{1}H to ^{13}C spins via cross-polarization in the solid state. The latter concept was demonstrated for intramolecular[19] and intermolecular[20] ^{1}H-to-^{13}C hyperpolarization transfers, and the ^{13}C exponential build-up time was shortened to 810 s. The final steps of d-DNP is a rapid (on the time scale of a few seconds) dissolution and warming of the cold HP sample, and the sample transfer from the DNP hyperpolarizer magnet to the imager or NMR magnet. The resulting HP ^{13}C contrast agent is typically administered to a subject via IV injection within seconds after dissolution.

Many ^{13}C- and ^{15}N-enriched biomolecules have been hyperpolarized with d-DNP, including 1-^{13}C-pyruvic acid,[8, 21] ^{13}C-bicarbonate,[22] 1-^{13}C-fumarate,[23] 5-^{13}C-glutamine,[24] ^{15}N-choline,[17] and others. The use of long-lived singlet states was also demonstrated in a ^{13}C-^{13}C spin pair in diacetyl[18b] hyperpolarized by d-DNP.[18b] Furthermore, recent advanced efforts of molecular deuteration enabled d-DNP and *in vivo* use of ^{13}C-choline[25] and ^{13}C-glucose,[26] which have significantly shorter T_1s in their non-deuterated forms. 1-^{13}C-pyruvic acid, which probes glycolysis *in vivo*,[21] is the leading ^{13}C HP contrast agent, and is already being evaluated by FDA-approved prostate cancer clinical trials in men[4, 27] work that is also fueled by the advent of the clinical scale d-DNP hyperpolarizer with a sterile path.[28] The DNP approach is also amenable to hyperpolarized silicon nanoparticles, where experiments have exploited the high biocompatibility, surface "functionalizability", and ultra-long ^{29}Si T_1's (~ 40 min.) of these systems[14] to perform HP ^{29}Si MRI *in vivo*.[14b] It should also be pointed out that the ^{29}Si DNP process is conducted in the solid state as a powder, without the need for the addition of radicals (because surface defects provide the unpaired electrons needed for DNP) or glassing agents.[14b] Finally, we should add briefly that potential clinical applications of DNP are not limited strictly to d-DNP: For example, in *ex situ* Overhauser DNP (ODNP), target molecules can be flowed continuously through beds containing immobilized radical species, allowing the target spins to be partially hyperpolarized with microwave application and subsequent delivery of the pure agent to the subject. In one recent example, the potential

Author Manuscript Author Manuscript Author Manuscript Author Manuscript

utility of ODNP-polarized water for performing perfusion MRI was demonstrated in a rat model.[29]

Spin-Exchange Optical Pumping (SEOP)

Spin-exchange optical pumping can be used to generate large quantities of hyperpolarized noble gases (^{3}He, ^{129}Xe, ^{83}Kr, etc.) with high nuclear spin polarization for biomedical applications [12b, 12c, 12f, 30]—approaching unity for ^{129}Xe[5b, 31] and ^{3}He.[32] Creation of hyperpolarized noble gases via SEOP generally requires a high-power circularly-polarized laser and an optical cell (Figure 2a) containing the target noble gas of interest, buffer gas (typically ^{4}He and/or N_2), and a small quantity of alkali metal that is partially vaporized by heating. While one could argue that the origins of the first step of SEOP—*optical pumping* of the alkali metal atoms (Figure 2b)—began with Zeeman's studies of sodium vapor,[1] it was Kastler who found that the vapor of another alkali metal—rubidium—could become *electronically* spin-polarized when placed in a magnetic field and illuminated with resonant circularly polarized light.[33] Bouchiat, Carver, and others later showed that the electronic spin polarization of the alkali metal vapor could be transferred to *nuclear* spins of noble gas atoms like ^{3}He and ^{129}Xe during gas-phase collisions.[34] This second step of SEOP, termed *spin-exchange* (Figure 2c), allows the nuclear spin polarization of the noble gas to ultimately approach that of the alkali metal electrons, provided that the spin-exchange rate greatly exceeds the noble gas spin-destruction rate (effectively, $1/T_1$). Various stand-alone apparatus designs for SEOP have been developed over the years—particularly for ^{129}Xe[3, 5b, 35]; such so-called "Xe hyperpolarizers" are capable of generating clinically-relevant quantities of HP^{129}Xe with polarizations now approaching unity.

Of the NMR-active noble gas isotopes, ^{3}He has the greatest γ value (and hence highest per-atom detection sensitivity), and until recently it was the easiest to achieve the highest levels of polarization. However, its natural abundance is extremely low, and instead is typically obtained from tritium decay; thus its future in biomedicine may be limited by the worldwide shortage of this effectively non-renewable resource.[36] The quadrupolar isotopes (I>1/2, ^{21}Ne, ^{83}Kr, and ^{131}Xe) can also be hyperpolarized (albeit not to the same extent) but generally suffer from inherently faster T_1 relaxation; of these, ^{83}Kr arguably shows the greatest promise for biomedical applications, where its quadrupolar interaction may embody a complementary, surface-sensitive source of contrast compared to its spin-1/2 brethren.[30] Nevertheless, ^{129}Xe—being spin-1/2, relatively inexpensive, naturally abundant, and amenable to near-unity hyperpolarization, while also possessing interesting properties (see below)—will be the primary focus of the present discussion.

Xenon, while almost chemically inert, has a predilection for transiently associating with a variety of substances and surfaces, including host-guest forming "cage" compounds, nanoporous materials, membranes, and various proteins.[12b, 37] Xe also exhibits a reasonable amount of solubility in blood and other living tissues.[38] Indeed, Xe's general biomedical applications are well-documented: it is a functional anesthetic;[39] recently, it has also been implicated as a possible performance-enhancing drug as well as a potential treatment for PTSD patients.[40] Importantly here, ^{129}Xe also possesses an extraordinarily sensitive chemical shift—causing its resonance frequency to vary over 200 ppm simply from

Author Manuscript Author Manuscript Author Manuscript Author Manuscript

being physically associated with different chemical environments—enabling HP ^{129}Xe to be a sensitive "spin-spy" of its local surroundings. HP ^{129}Xe can also be a *source* of hyperpolarization for other systems using various polarization-transfer techniques,[41] although such approaches to date have not commonly been exploited for biomedical applications. Instead, biomedical ^{129}Xe MRS/MRI typically exploits xenon location—as originally demonstrated in the first biomedical application of HP Xe, void space imaging in excised mouse lungs[42]—density, motion (e.g. apparent local diffusion or exchange), chemical shift, and/or spin relaxation. One intriguing approach exploits Xe's fondness for cage compounds and its chemical shift and exchange properties in order to directly encode specific biomolecular information onto the ^{129}Xe signal using so-called Xe biosensors.[43] These agents are comprised of a Xe-binding cage compound (typically a cryptophane derivative[44]) covalently tethered to some bioanalyte; if the Xe biosensor binds to a targeted protein, then the chemical shift of the bound ^{129}Xe changes, allowing it to be resolved from both Xe in unbound cages and Xe freely floating in solution. The potential for using such agents *in vivo* has been strengthened by the "hyperCEST" (hyperpolarized chemical exchange saturation transfer) approach, where the presence of even a small amount of Xe-occupied cages bound to their biomolecular targets can be encoded onto the easier-to-detect signal from Xe in the bulk environment. As another example, Branca and co-workers demonstrated the promise of a different but clever approach to achieving molecular imaging using HP gases:[45] with the goal of visualizing lung metastases, cancer cells are first targeted by superparamagnetic nanoparticles (SPIONs) surface-functionalized with cancer-binding molecules, and then the lung space is imaged with HP noble gases (here, ^{3}He) to identify any regions where the HP signal had been washed out by the local presence of SPIONs. Regardless of the experiment and ^{129}Xe detection modality, HP Xe can be delivered to the subject via inhalation[12b, 12c, 12f, 30] or via the administration of Xe-saturated biologically tolerable solutions.[46]

ParaHydrogen Induced Polarization (PHIP)

The PHIP method of hyperpolarization relies on fast chemical reactions that enable pairwise addition of *p*-H_2 across unsaturated chemical bonds—typically C=C or C≡C bonds adjacent to ^{13}C carboxyl or ^{15}N[49] nuclei. Bowers and Weitekamp demonstrated that the nuclear spin singlet state of parahydrogen molecules can be converted into observable magnetization arising from the magnetically inequivalent positions at the site of hydrogenation with *p*-H_2,[50] Figure 3c. The chemical reaction of pairwise *p*-H_2 addition should be performed faster than the nuclear spin relaxation of the nascent protons. Goldman, Spiess, Bargon and Golman later demonstrated that the nascent proton hyperpolarization can be transferred to carboxyl ^{13}C nuclei to yield HP ^{13}C contrast agents in seconds using either RF-based or field-cycling hyperpolarization-transfer approaches, respectively (Figure 3c).[51] The speed of the PHIP method is one of its main advantages, while the requirement for an unsaturated molecular PHIP precursor with appropriate asymmetry is a significant limitation for biological applications. Moreover, while RF-based PHIP polarization transfer (Figure 3c) benefits from deuteration of the molecular precursor, it also further increases the design complexity for the molecular PHIP precursor.[52] Nevertheless, a number of potentially useful biomolecules were successfully hyperpolarized using PHIP, including 1-^{13}C-succinic

Author Manuscript Author Manuscript Author Manuscript Author Manuscript

acid,[53] 1-^{13}C-phospholactate,[52, 54] tetrafluoropropyl 1-^{13}C-propionate,[55] ^{15}N-propargylglycine,[49] ^{13}C-glucose derivative,[56] and others. Despite the synthetic challenges, new concepts of using –OH protection in -C=C-O-R motifs have significantly expanded the reach of molecular targets for PHIP,[54, 57] because the protecting group can be removed after PHIP either metabolically[52, 54, 58] or synthetically.[57]

The PHIP hydrogenation procedure has often been conducted conventionally with homogeneous Rh(I) based catalysts (e.g. Wilkinson's catalyst[59]), which more recently have been replaced by water-soluble bisphosphine Rh(I) catalysts—enabling biomedical use *in vivo*.[51a, 53a, 55] However, Koptyug and co-workers[60] demonstrated that heterogeneous catalysts including supported metal nanoparticles of Rh and other metals,[12e] which despite ostensibly relying on predominantly non-molecular mechanisms of hydrogenation, can in fact yield a significant fraction of the hydrogenated product via effectively "pairwise" addition of *p*-H_2—resulting in HP product. The 'HET-PHIP' concept was demonstrated in the creation of HP propane and other gases,[12e] substances which in principle can be used directly in biomedical applications like gas MRI (similar to HP noble gases discussed above). HP propane with P_H>0.01 has already been demonstrated to be useful for high-resolution 3D MRI in phantoms.[61] These new supported metal catalysts can also be applied for heterogeneous PHIP at the liquid-solid interface,[12e] and may enable the production of pure aqueous HP contrast agents—agents that have already been previously prepared via homogeneous catalysis and shown to be promising targets for biomedical applications.[52, 53b, 53c, 54–55, 58] The potential realization of this emerging concept would additionally allow recycling the catalyst—making PHIP a truly low-cost, high-throughput, sustainable, and scalable HP technique.

As stated above, PHIP relies on the pure spin order of the singlet state of *p*-H_2;[50] but first, the spin order must be generated. H_2 molecules can exist in both para- (spin-0) and ortho- (spin-1) states, with an energy difference of ~170 K[63]—resulting in a statistical 3:1 (ortho:para) spin isomer distribution at normal "high-temperature" conditions. However, because the *p*-H_2 singlet corresponds to the lower-energy state of these two spin isomers, 'normal' H_2 gas can be converted to preferentially favor the *p*-H_2 spin isomer by cooling the gas to cryogenic temperatures, Figure 3b. The process of para⇔ortho interconversion is normally very slow (on the time scale of months if not longer)[64] but can be significantly accelerated through the use of a catalyst in the *p*-H_2 generating equipment (Figure 3a):[65] When H_2 gas passes through the cold catalyst-filled chamber (Figure 3a), it is rapidly converted to the local equilibrium *p*-H_2 fraction determined by the low temperature of the cryogenically-cooled chamber (Figure 3b). The exiting *p*-H_2 is then warmed to room temperature (RT), and is typically stored in an aluminum tank for PHIP and SABRE applications. While the enriched *p*-H_2 is thermodynamically less favorable at RT, it is effectively kinetically trapped in the para- state, and can be stored for weeks or months in the absence of paramagnetic impurities such as O_2. It should also be noted that *p*-H_2 is NMR-invisible, because its net spin is zero; perhaps ironically, it is the *o*-H_2 spin isomer that provides the NMR signal for H_2 gas. This property is conveniently used to quantify the percentage of *p*-H_2 enrichment using conventional high-resolution NMR.[64, 66]

Author Manuscript Author Manuscript Author Manuscript Author Manuscript

Signal Amplification by Reversible Exchange (SABRE)

SABRE[11, 62] is a relatively new PHIP-based hyperpolarization technique pioneered by Duckett and co-workers in 2009. However, while SABRE relies on *p*-H_2 exchange on a metal complex, it differs from traditional PHIP in that the *p*-H_2 does not chemically react with the substrate molecule to be hyperpolarized. Indeed, in SABRE the substrate also exchanges rapidly between the bulk solution environment and the organometallic catalyst complex, allowing spin order to be spontaneously transferred from exchangeable ('para-')hydride to the substrate molecule at low[62] and high[67] magnetic fields (Figure 3d; believed to be mediated by scalar couplings and dipolar cross-relaxation, respectively). The exchangeable organometallic catalyst is the key element of SABRE hyperpolarization method,[68] and the most effective iridium N-heterocyclic carbene complexes[69] have been used to achieve substrate hyperpolarization with *P* as high as ~8%. This method, previously demonstrated on pyridine and nicotinamide, has already been efficiently expanded to other biologically relevant molecules such as the tuberculosis drugs pyrazinamide and isoniazid.[70] While the vast majority of SABRE studies are carried out in organic solvents, the first efforts to achieve SABRE hyperpolarization in aqueous/organic[71] and purely aqueous media[72] are promising—particularly given the fact that SABRE, barely five years old, is still very much in its infancy. Moreover, the first demonstration of heterogeneous SABRE was recently reported,[73] ultimately paving the way to applications where the SABRE catalysts—consisting of metal complexes covalently tethered to solid supports—may be recycled, and pure solutions of HP contrast agent may be produced. Once combined with SABRE in aqueous media, this method may in fact embody a cheap, efficient, and scalable approach to quickly produce large quantities of pure HP contrast agents on demand. If realized, this would provide a clear strength of the SABRE approach.

Detection of Hyperpolarized Contrast Media

Because HP magnetization for a given 'batch' of HP agent is transient and cannot be regenerated in biomedical applications, it irrevocably decays to its equilibrium value—typically several orders of magnitude weaker than that embodied by the HP state; moreover, each acquisition RF pulse "uses up" some of the hard-won HP magnetization. On the other hand, the bright signal provided by the HP agent obviates the need for built-in delays that may otherwise be required to allow equilibrium spin polarization to refresh after each acquisition. As a result of these facts, most conventional NMR and MRI pulse sequences cannot be readily used for HP media without at least some modification. Importantly, an additional source of signal decay for an HP contrast agent in living tissues is its metabolism. For example, *in vivo* injection of HP 1-^{13}C-pyruvate leads to its rapid enzymatic conversion to HP 1-^{13}C-lactate and 1-^{13}C-alanine, Figure 4a.[21a] Such processes highlight a clear strength of HP MRI, as both contrast agent uptake *and* its metabolism can be detected and quantified—thereby providing an additional layer of molecular information. However, the biochemical change of the signal source also represents a challenge for MRI pulse sequence development, because the simultaneous presence of HP ^{13}C signals from multiple species complicates image encoding and reconstruction. This problem is resolved through the addition of the *spectroscopic* dimension to the spatial dimensions of MRI pulse sequences through an established method called Chemical Shift Imaging (CSI), which enables

Author Manuscript Author Manuscript Author Manuscript Author Manuscript

detection of spectra from individual voxels[21a, 74] that can later be used to reconstruct metabolic maps of HP species—i.e. originally injected HP contrast agent (pyruvate) and its products (lactate and alanine)—as shown in Figure 4a. Furthermore, more advanced pulse sequences with frequency-selective RF pulses can be designed to sample only metabolites (the products of interest) rather than the original contrast agent, which also serves to minimize polarization losses due to RF excitation.[75]

HP RF pulse sequences rarely use full (90° flip-angle) or nearly full NMR signal excitation (with an exception of state-state free precession (ssfp) sequences, where gradient refocusing is utilized[66, 75c, 76]), because the HP magnetization is finite and non-renewable; the detected magnetization is proportional to the sine of the applied RF pulse angle, whereas the residual magnetization is proportional to the cosine of the applied RF pulse angle (Figure 4c). As a result, the use of low tipping-angle excitation RF pulses (i.e. just a few degrees) is highly advantageous for HP MRI sequences, because doing so retains most of the available HP magnetization for subsequent acquisitions (allowing the HP but finite magnetization to be "metered out" as efficiently as possible). Moreover, unlike conventional MR, where a recovery time interval in the pulse sequence is needed to re-establish the equilibrium nuclear spin polarization, HP MR pulse sequences no longer need this recovery interval because HP magnetization is created outside of—and not by—the imaging magnet (Figure 4d). Thus, a HP pulse sequence train needs only to contain the encoding and detecting elements, thereby providing significant imaging acceleration—with repetition times on the order of a few ms, and entire 3D scanning times on the order of seconds.[5b] However even with small RF tipping angles, if the excitation RF pulse width is kept fixed, the decaying HP magnetization will yield progressively reduced MR signal during the pulse sequence train due to the previous pulsing, as well as T_1 and other polarization losses. This shortcoming can be mitigated through the use of pulse sequences with progressively increasing RF pulse tipping-angle to maintain (ideally) the same induced MR signal throughout the progression of the sequence train, Figure 4d.

Many HP imaging *applications* require fast scanning speed. For example, performing a 3D MRI lung scan on a single patient breath hold restricts the scanning duration to just a few seconds. Imaging scanning speed can be additionally significantly accelerated through the use of compressed sensing,[75a, 76] where only a fraction of *k*-space is sampled, which can lead to a corresponding several-fold reduction in total scan time.

Biomedical Translation

To date, a number of HP contrast agents have been developed and tested in animal models of human diseases, human subjects, or both, including: HP 1-^{13}C-pyruvate, reporting on upregulated glycolysis in cancers[21b, 77]; HP ^{129}Xe and ^{3}He, reporting on pulmonary function through images of lung ventilation, diffusion maps, and gas perfusion[12c] as well as Xe distribution *in vivo*;[78] HP 1-^{13}C-succinate[53c] and 1-^{13}C-fumarate,[23] reporting on TCA cycle metabolism; HP 5-^{13}C-glutamine, reporting on elevated glutaminolysis in cancer; HP ^{29}Si nanoparticles[14] and others—with more on the way. However, clinical biomedical translation of the fundamental advances in the chemistry and physics of HP MR requires several components: (i) a clinical-scale hyperpolarizer capable of producing HP

Author Manuscript Author Manuscript Author Manuscript Author Manuscript

agent doses suitable (quantity, purity, sterility, etc.) for administration to patients; (ii) regulatory approvals from government agencies and local institutions; and (iii) a MRI scanner capable of multi-nuclear (^{1}H as well as ^{13}C, ^{129}Xe, etc.) detecting capabilities—including specialized RF coils, custom RF pulse sequences, etc.; and of course (iv) trained, dedicated personnel capable of navigating/operating i-iii above. Despite these requirements and challenges, a number of clinical or pre-clinical human trials are underway—or already completed—with HP ^{129}Xe (produced via SEOP) and HP ^{13}C (produced via d-DNP). Examples of clinical research HP MRI are provided in Figure 5. Figure 5a shows 2 selected slices of 3D functional pulmonary ventilation imaging scan using HP ^{129}Xe. HP ^{129}Xe was inhaled by a healthy volunteer, and the entire 3D MRI exam was conducted in less than 5 seconds on a single breath hold.[5b, 35e] Bright signals are obtained from the void spaces of the lungs, as the enormous signal provided by the HP ^{129}Xe more than outweighs the low spin density of the gas phase. Moreover, the background signal from surrounding tissues is non-existent due to the virtual absence of Xe naturally occurring in the body. The potential utility of two other features of ^{129}Xe—its highly sensitive chemical shift and its tendency to be rapidly absorbed by living tissues—is demonstrated in Figure 5b. First, a HP ^{129}Xe NMR spectrum from the brain of a healthy human subject inhaling HP Xe (left) is shown to exhibit five different peaks, tentatively assigned to red blood cells, blood plasma, grey matter, white matter, and lipid, respectively.[79] The ability to selectively create a spatial map of one of these resonances/compartments—here, that of ^{129}Xe residing in red blood cells—is demonstrated in the corresponding image (right), where the strongest ^{129}Xe signals likely originating from the brain's Circle of Willis.[79] Figure 5c shows examples taken from a Magnetic Resonance Spectroscopic Imaging (MRSI) study using intravenous injection of HP 1-^{13}C-pyruvate.[27] The injected HP 1-^{13}C-pyruvate is rapidly converted to HP 1-^{13}C-lactate by LDH (see Figure 4a), and the ratio 1-^{13}C-lactate/1-^{13}C-pyruvate[77b] (measured as the intensity ratio of HP signals of HP 1-^{13}C-lactate and 1-^{13}C-pyruvate in the spectroscopic domain of MRSI; see Figure 4a) serves as a metabolic imaging biomarker of prostate cancer. This ratio of HP signals is presented as a false-color overlay image co-registered with a conventional T_2-weighted MRI of prostate (grey-scale), and is shown for three prostate cancer subjects. Note that the tumors are very difficult to detect on conventional proton MRI images (top row of Figure 5b), while the metabolic molecular imaging offers additional contrast mechanism that can delineate diseased tissues from healthy ones by "lighting up" regions with potentially pathological metabolism.

Conclusions

HP contrast agents with biomedical relevance can be now prepared by several hyperpolarization techniques, including: d-DNP, SEOP, PHIP, and SABRE. These techniques significantly increase nuclear spin polarization and hence MR sensitivity by orders of magnitude—permitting new biomedical applications including functional and metabolic molecular imaging. HP contrast agents hold great promise to enable a broad range of new imaging biomarkers for molecular imaging of deadly diseases such as cancer, COPD, emphysema, and others. Compared to Positron Emission Tomography (PET), which is the leading molecular imaging modality, HP MRI offers advantages of (i) being non-radioactive and non-ionizing, and (ii) potentially providing more metabolic information rather than only

Author Manuscript Author Manuscript Author Manuscript Author Manuscript

reporting on contrast agent uptake, and (iii) very short (few seconds) imaging scan with possibility of multiple same-day examinations.[80] Furthermore, some hyperpolarization techniques (PHIP and SABRE) and detection methods (low-field MRI) potentially offer additional advantages of speed, throughput and cost. While the seeds of most hyperpolarization techniques were planted decades ago, most have matured for biomedical applications only during the last decade. Indeed, there is a tremendous room for innovation in fundamental physics, chemistry, biochemistry, and engineering that could significantly improve or even revolutionize this emerging area of molecular imaging.

Acknowledgments

We thank for funding support NIH 1R21EB018014, National Science Foundation CHE - 1416268, and DoD CDMRP Breast Cancer Program Era of Hope Award W81XWH-12-1-0159/BC112431.

References

1. Zeeman P. Nature. 1897; 55:347.
2. Carver TR, Slichter CP. Phys Rev. 1953; 92:212–213.
3. Nikolaou P, Coffey AM, Barlow MJ, Rosen M, Goodson BM, Chekmenev EY. Anal Chem. 2014; 86:8206–8212. [PubMed: 25008290]
4. Kurhanewicz J, Vigneron DB, Brindle K, Chekmenev EY, Comment A, Cunningham CH, DeBerardinis RJ, Green GG, Leach MO, Rajan SS, Rizi RR, Ross BD, Warren WS, Malloy CR. Neoplasia. 2011; 13:81–97. [PubMed: 21403835]
5. a) Muradyan I, Butler JP, Dabaghyan M, Hrovat M, Dregely I, Ruset I, Topulos GP, Frederick E, Hatabu H, Hersman WF, Patz S. J Magn Reson Imaging. 2013; 37:457–470. [PubMed: 23011916] b) Nikolaou P, Coffey AM, Walkup LL, Gust BM, Whiting N, Newton H, Barcus S, Muradyan I, Dabaghyan M, Moroz GD, Rosen M, Patz S, Barlow MJ, Chekmenev EY, Goodson BM. Proc Natl Acad Sci U S A. 2013; 110:14150–14155. [PubMed: 23946420]
6. Tsai LL, Mair RW, Rosen MS, Patz S, Walsworth RL. J Magn Reson. 2008; 193:274–285. [PubMed: 18550402]
7. Coffey AM, Truong ML, Chekmenev EY. J Magn Reson. 2013; 237:169–174. [PubMed: 24239701]
8. Ardenkjaer-Larsen JH, Fridlund B, Gram A, Hansson G, Hansson L, Lerche MH, Servin R, Thaning M, Golman K. Proc Natl Acad Sci U S A. 2003; 100:10158–10163. [PubMed: 12930897]
9. Walker TG, Happer W. Rev Mod Phys. 1997; 69:629–642.
10. Eisenschmid TC, Kirss RU, Deutsch PP, Hommeltoft SI, Eisenberg R, Bargon J, Lawler RG, Balch AL. J Am Chem Soc. 1987; 109:8089–8091.
11. Adams RW, Aguilar JA, Atkinson KD, Cowley MJ, Elliott PIP, Duckett SB, Green GGR, Khazal IG, Lopez-Serrano J, Williamson DC. Science. 2009; 323:1708–1711. [PubMed: 19325111]
12. a) Gallagher FA, Kettunen MI, Brindle KM. Prog Nucl Mag Res Sp. 2009; 55:285–295.b Goodson BM. J Magn Reson. 2002; 155:157–216. [PubMed: 12036331] c) Mugler JP, Altes TA. J Magn Reson Imaging. 2013; 37:313–331. [PubMed: 23355432] d) Gloggler S, Colell J, Appelt S. J Magn Reson. 2013; 235:130–142. [PubMed: 23932399] e) Kovtunov KV, Zhivonitko VV, Skovpin IV, Barskiy DA, Koptyug IV. Top Curr Chem. 2013; 338:123–180. [PubMed: 23097028] f) Walkup LL, Woods JC. NMR Biomed. 201410.1002/nbm.3151g) Green RA, Adams RW, Duckett SB, Mewis RE, Williamson DC, Green GGR. Prog Nucl Mag Res Sp. 2012; 67:1–48.h) Lee JH, Okuno Y, Cavagnero S. J Magn Reson. 2014; 241:18–31. [PubMed: 24656077]
13. McCarney ER, Armstrong BD, Lingwood MD, Han S. Proc Natl Acad Sci U S A. 2007; 104:1754–1759. [PubMed: 17264210]
14. a) Aptekar JW, Cassidy MC, Johnson AC, Barton RA, Lee M, Ogier AC, Vo C, Anahtar MN, Ren Y, Bhatia SN, Ramanathan C, Cory DG, Hill AL, Mair RW, Rosen MS, Walsworth RL, Marcus CM. ACS Nano. 2009; 3:4003–4008. [PubMed: 19950973] b) Cassidy MC, Chan HR, Ross BD, Bhattacharya PK, Marcus CM. Nat Nanotechnol. 2013; 8:363–368. [PubMed: 23644571]

Author Manuscript Author Manuscript Author Manuscript Author Manuscript

15. Chekmenev EY, Norton VA, Weitekamp DP, Bhattacharya P. J Am Chem Soc. 2009; 131:3164–3165. [PubMed: 19256566]
16. Pileio G, Carravetta M, Hughes E, Levitt MH. J Am Chem Soc. 2008; 130:12582–12583. [PubMed: 18729363]
17. Gabellieri C, Reynolds S, Lavie A, Payne GS, Leach MO, Eykyn TR. J Am Chem Soc. 2008; 130:4598–4599. [PubMed: 18345678]
18. a) Carravetta M, Levitt MH. J Am Chem Soc. 2004; 126:6228–6229. [PubMed: 15149209] b) Warren WS, Jenista E, Branca RT, Chen X. Science. 2009; 323:1711–1714. [PubMed: 19325112] c) Kovtunov KV, Truong ML, Barskiy DA, Koptyug IV, Waddell KW, Chekmenev EY. Chem Eur J. 2014; 20:14629–14632. [PubMed: 25263795] d) Kovtunov KV, Truong ML, Barskiy DL, Salnikov OG, Bukhtiyarov VI, Coffey AM, Waddell KW, Koptyug IV, Chekmenev EY. J Phys Chem C. 201410.1021/jp508719n
19. Bornet A, Melzi R, Perez Linde AJ, Hautle P, van den Brandt B, Jannin S, Bodenhausen G. J Phys Chem Lett. 2013; 4:111–114.
20. Vuichoud B, Milani J, Bornet A, Melzi R, Jannin S, Bodenhausen G. J Phys Chem B. 2014; 118:1411–1415. [PubMed: 24397585]
21. a) Golman K, in't Zandt R, Thaning M. Proc Natl Acad Sci U S A. 2006; 103:11270–11275. [PubMed: 16837573] b) Day SE, Kettunen MI, Gallagher FA, Hu DE, Lerche M, Wolber J, Golman K, Ardenkjaer-Larsen JH, Brindle KM. Nat Med. 2007; 13:1382–1387. [PubMed: 17965722]
22. Gallagher FA, Kettunen MI, Day SE, Hu DE, Ardenkjaer-Larsen JH, in't Zandt R, Jensen PR, Karlsson M, Golman K, Lerche MH, Brindle KM. Nature. 2008; 453:940–U973. [PubMed: 18509335]
23. Gallagher FA, Kettunen MI, Hu DE, Jensen PR, in't Zandt R, Karlsson M, Gisselsson A, Nelson SK, Witney TH, Bohndiek SE, Hansson G, Peitersen T, Lerche MH, Brindle KM. Proc Natl Acad Sci U S A. 2009; 106:19801–19806. [PubMed: 19903889]
24. Gallagher FA, Kettunen MI, Day SE, Lerche M, Brindle KM. Magn Reson Med. 2008; 60:253–257. [PubMed: 18666104]
25. a) Kumagai K, Kawashima K, Akakabe M, Tsuda M, Abe T, Tsuda M. Tetrahedron. 2013; 69:3896–3900.b) Friesen-Waldner LJ, Wade TP, Thind K, Chen AP, Gomori JM, Sosna J, McKenzie CA, Katz-Brull R. J Magn Reson Imaging. 201410.1002/jmri.24659c) Nonaka H, Hata R, Doura T, Nishihara T, Kumagai K, Akakabe M, Tsuda M, Ichikawa K, Sando S. Nat Commun. 2013:4.
26. a) Rodrigues TB, Serrao EM, Kennedy BWC, Hu DE, Kettunen MI, Brindle KM. Nat Med. 2014; 20:93–97. [PubMed: 24317119] b) Harris T, Degani H, Frydman L. NMR Biomed. 2013; 26:1831–1843. [PubMed: 24115045]
27. Nelson SJ, Kurhanewicz J, Vigneron DB, Larson PEZ, Harzstark AL, Ferrone M, van Criekinge M, Chang JW, Bok R, Park I, Reed G, Carvajal L, Small EJ, Munster P, Weinberg VK, Ardenkjaer-Larsen JH, Chen AP, Hurd RE, Odegardstuen LI, Robb FJ, Tropp J, Murray JA. Sci Transl Med. 2013; 5:198ra108.
28. Ardenkjaer-Larsen JH, Leach AM, Clarke N, Urbahn J, Anderson D, Skloss TW. NMR Biomed. 2011; 24:927–932. [PubMed: 21416540]
29. Lingwood MD, Siaw TA, Sailasuta N, Abulseoud OA, Chan HR, Ross BD, Bhattacharya P, Han S. Radiology. 2012; 265:418–425. [PubMed: 22996746]
30. Lilburn D, Pavlovskaya GE, Meersmann T. J Magn Reson. 2012; 229:173–186. [PubMed: 23290627]
31. Freeman MS, Emami K, Driehuys B. Phys Rev A. 2014; 90:023406. [PubMed: 25400489]
32. Chen WC, Gentile TR, Ye Q, Walker TG, Babcock E. J Appl Phys. 2014; 116:6.
33. Kastler A. J Phys Radium. 1950; 11:255–265.
34. Bouchiat MA, Carver TR, Varnum CM. Phys Rev Lett. 1960; 5:373–375.
35. a) Driehuys B, Cates GD, Miron E, Sauer K, Walter DK, Happer W. Appl Phys Lett. 1996; 69:1668–1670.b) Swanson SD, Rosen MS, Coulter KP, Welsh RC, Chupp TE. Magn Reson Med. 1999; 42:1137–1145. [PubMed: 10571936] c) Nikolaou P, Coffey AM, Ranta K, Walkup LL, Gust B, Barlow MJ, Rosen MS, Goodson BM, Chekmenev EY. J Phys Chem B. 2014; 118:4809–4816.

Author Manuscript Author Manuscript Author Manuscript Author Manuscript

[PubMed: 24731261] d) Nikolaou P, Coffey AM, Walkup LL, Gust B, LaPierre C, Koehnemann E, Barlow MJ, Rosen MS, Goodson BM, Chekmenev EY. J Am Chem Soc. 2014; 136:1636–1642. [PubMed: 24400919] e) Nikolaou P, Coffey AM, Walkup LL, Gust BM, Whiting NR, Newton H, Muradyan I, Dabaghyan M, Ranta K, Moroz G, Patz S, Rosen MS, Barlow MJ, Chekmenev EY, Goodson BM. Magn Reson Imaging. 2014; 32:541–550. [PubMed: 24631715] f) Ruset IC, Ketel S, Hersman FW. Phys Rev Lett. 2006; 96:053002. [PubMed: 16486926] g) Norquay G, Parnell SR, Xu XJ, Parra-Robles J, Wild JM. J Appl Phys. 2013; 113:9.

36. Shea DA, Morgan D. CRS Report for Congress. 2010
37. a) Dubois L, Da Silva P, Landon C, Huber JG, Ponchet M, Vovelle F, Berthault P, Desvaux H. J Am Chem Soc. 2004; 126:15738–15746. [PubMed: 15571396] b) Chen L, Reiss PS, Chong SY, Holden D, Jelfs KE, Hasell T, Little MA, Kewley A, Briggs ME, Stephenson A, Thomas KM, Armstrong JA, Bell J, Busto J, Noel R, Liu J, Strachan DM, Thallapally PK, Cooper AI. Nat Mater. 2014 advance online publication. 10.1038/nmat4035
38. Chen RYZ, Fan FC, Kim S, Jan KM, Usami S, Chien S. J Appl Physiol. 1980; 49:178–183. [PubMed: 7400000]
39. Kennedy RR, Stokes JW, Downing P. Anaesth Intensive Care. 1992; 20:66–70. [PubMed: 1319119]
40. Meloni EG, Gillis TE, Manoukian J, Kaufman MJ. PLoS One. 2014; 9:e106189. [PubMed: 25162644]
41. a) Bowers CR, Long HW, Pietrass T, Gaede HC, Pines A. Chem Phys Lett. 1993; 205:168–170.b) Navon G, Song YQ, Room T, Appelt S, Taylor RE, Pines A. Science. 1996; 271:1848–1851.c) Cherubini A, Payne GS, Leach MO, Bifone A. Chem Phys Lett. 2003; 371:640–644.d) Lisitza N, Muradian I, Frederick E, Patz S, Hatabu H, Chekmenev EY. J Chem Phys. 2009; 131:044508. [PubMed: 19655895]
42. Albert MS, Cates GD, Driehuys B, Happer W, Saam B, Springer CS, Wishnia A. Nature. 1994; 370:199–201. [PubMed: 8028666]
43. a) Spence MM, Rubin SM, Dimitrov IE, Ruiz EJ, Wemmer DE, Pines A, Yao SQ, Tian F, Schultz PG. Proc Natl Acad Sci U S A. 2001; 98:10654–10657. [PubMed: 11535830] b) Schroder L, Lowery TJ, Hilty C, Wemmer DE, Pines A. Science. 2006; 314:446–449. [PubMed: 17053143] c) Schroder L. Phys Medica. 2013; 29:3–16.d) Rose HM, Witte C, Rossella F, Klippel S, Freund C, Schröder L. Proc Natl Acad Sci U S A. 2014; 111:11697–11702. [PubMed: 25071165] e) Delacour L, Kotera N, Traore T, Garcia-Argote S, Puente C, Leteurtre F, Gravel E, Tassali N, Boutin C, Leonce E, Boulard Y, Berthault P, Rousseau B. Chem Eur J. 2013; 19:6089–6093. [PubMed: 23494947] f) Shapiro MG, Ramirez RM, Sperling LJ, Sun G, Sun J, Pines A, Schaffer DV, Bajaj VS. Nat Chem. 2014; 6:629–634. [PubMed: 24950334]
44. Brotin T, Dutasta JP. Chem Rev. 2009; 109:88–130. [PubMed: 19086781]
45. Branca RT, Cleveland ZI, Fubara B, Kumar CSSR, Maronpot RR, Leuschner C, Warren WS, Driehuys B. Proc Natl Acad Sci U S A. 2010; 107:3693–3697. [PubMed: 20142483]
46. a) Goodson BM. Concept Magnetic Res. 1999; 11:203–223.b Cherubini A, Bifone A. Prog Nucl Mag Res Sp. 2003; 42:1–30.c) Acosta RH, Blümler P, Münnemann K, Spiess HW. Prog Nucl Mag Res Sp. 2012; 66:40–69.
47. Whiting N, Eschmann NA, Goodson BM, Barlow MJ. Phys Rev A. 2011; 83:6.
48. Saha I, Nikolaou P, Whiting N, Goodson BM. Chem Phys Lett. 2006; 428:268–276.
49. Reineri F, Viale A, Ellena S, Alberti D, Boi T, Giovenzana GB, Gobetto R, Premkumar SSD, Aime S. J Am Chem Soc. 2012; 134:11146–11152. [PubMed: 22663300]
50. Bowers CR, Weitekamp DP. Phys Rev Lett. 1986; 57:2645–2648. [PubMed: 10033824]
51. a) Golman K, Axelsson O, Johannesson H, Mansson S, Olofsson C, Petersson JS. Magn Reson Med. 2001; 46:1–5. [PubMed: 11443703] b) Goldman M, Johannesson H. C R Physique. 2005; 6:575–581.c) Cai C, Coffey AM, Shchepin RV, Chekmenev EY, Waddell KW. J Phys Chem B. 2013; 117:1219–1224. [PubMed: 23214962] d) Haake M, Natterer J, Bargon J. J Am Chem Soc. 1996; 118:8688–8691.e) Roth M, Koch A, Kindervater P, Bargon J, Spiess HW, Muennemann K. J Magn Reson. 2010; 204:50–55. [PubMed: 20207180] f) Buljubasich L, Franzoni MB, Spiess HW, Munnemann K. J Magn Reson. 2012; 219:33–40. [PubMed: 22595295]

Author Manuscript Author Manuscript Author Manuscript Author Manuscript

52. Shchepin RV, Coffey AM, Waddell KW, Chekmenev EY. Anal Chem. 2014; 86:5601–5605. [PubMed: 24738968]
53. a) Bhattacharya P, Chekmenev EY, Perman WH, Harris KC, Lin AP, Norton VA, Tan CT, Ross BD, Weitekamp DP. J Magn Reson. 2007; 186:150–155. [PubMed: 17303454] b) Chekmenev EY, Hovener J, Norton VA, Harris K, Batchelder LS, Bhattacharya P, Ross BD, Weitekamp DP. J Am Chem Soc. 2008; 130:4212–4213. [PubMed: 18335934] c) Zacharias NM, Chan HR, Sailasuta N, Ross BD, Bhattacharya P. J Am Chem Soc. 2012; 134:934–943. [PubMed: 22146049]
54. Shchepin RV, Coffey AM, Waddell KW, Chekmenev EY. J Am Chem Soc. 2012; 134:3957–3960. [PubMed: 22352377]
55. Bhattacharya P, Chekmenev EY, Reynolds WF, Wagner S, Zacharias N, Chan HR, Bünger R, Ross BD. NMR Biomed. 2011; 24:1023–1028. [PubMed: 21538638]
56. Reineri F, Santelia D, Viale A, Cerutti E, Poggi L, Tichy T, Premkumar SSD, Gobetto R, Aime S. J Am Chem Soc. 2010; 132:7186–7193. [PubMed: 20441193]
57. Trantzschel T, Bernarding J, Plaumann M, Lego D, Gutmann T, Ratajczyk T, Dillenberger S, Buntkowsky G, Bargon J, Bommerich U. Phys Chem Chem Phys. 2012; 14:5601–5604. [PubMed: 22434387]
58. Shchepin RV, Pham W, Chekmenev EY. J Labelled Comp Radiopharm. 2014; 57:517–524. [PubMed: 24995802]
59. Bowers CR, Weitekamp DP. J Am Chem Soc. 1987; 109:5541–5542.
60. Kovtunov KV, Beck IE, Bukhtiyarov VI, Koptyug IV. Angew Chem Int Ed. 2008; 47:1492–1495.
61. Kovtunov KV, Barskiy DA, Coffey AM, Truong ML, Salnikov OG, Khudorozhkov AK, Inozemceva EA, Prosvirin IP, Bukhtiyarov VI, Waddell KW, Chekmenev EY, Koptyug IV. Chem Eur J. 2014; 20:11636–11639. [PubMed: 24961814]
62. Atkinson KD, Cowley MJ, Elliott PIP, Duckett SB, Green GGR, Lopez-Serrano J, Whitwood AC. J Am Chem Soc. 2009; 131:13362–13368. [PubMed: 19719167]
63. Goldman M, Johannesson H, Axelsson O, Karlsson M. C R Chimie. 2006; 9:357–363.
64. Feng B, Coffey AM, Colon RD, Chekmenev EY, Waddell KW. J Magn Reson. 2012; 214:258–262. [PubMed: 22188975]
65. Hövener JB, Chekmenev E, Harris K, Perman W, Robertson L, Ross B, Bhattacharya P. Magn Reson Mater Phy. 2009; 22:111–121.
66. Bhattacharya P, Harris K, Lin AP, Mansson M, Norton VA, Perman WH, Weitekamp DP, Ross BD. Magn Reson Mater Phy. 2005; 18:245–256.
67. a) Barskiy DA, Kovtunov KV, Koptyug IV, He P, Groome KA, Best QA, Shi F, Goodson BM, Shchepin RV, Coffey AM, Waddell KW, Chekmenev EY. J Am Chem Soc. 2014; 136:3322–3325. [PubMed: 24528143] b) Theis T, Truong M, Coffey AM, Chekmenev EY, Warren WS. J Magn Reson. 2014; 248:23–26. [PubMed: 25299767] c) Pravdivtsev AN, Yurkovskaya AV, Vieth H-M, Ivanov KL. Phys Chem Chem Phys. 201410.1039/C1034CP03765K
68. Lloyd LS, Asghar A, Burns MJ, Charlton A, Coombes S, Cowley MJ, Dear GJ, Duckett SB, Genov GR, Green GGR, Highton LAR, Hooper AJJ, Khan M, Khazal IG, Lewis RJ, Mewis RE, Roberts AD, Ruddlesden AJ. Catal Sci Tech. 201410.1039/C1034CY00464G
69. a) Cowley MJ, Adams RW, Atkinson KD, Cockett MCR, Duckett SB, Green GGR, Lohman JAB, Kerssebaum R, Kilgour D, Mewis RE. J Am Chem Soc. 2011; 133:6134–6137. [PubMed: 21469642] b) Vazquez-Serrano LD, Owens BT, Buriak JM. Inorg Chim Acta. 2006; 359:2786–2797.
70. Zeng H, Xu J, Gillen J, McMahon MT, Artemov D, Tyburn JM, Lohman JAB, Mewis RE, Atkinson KD, Green GGR, Duckett SB, van Zijl PCM. J Magn Reson. 2013; 237:73–78. [PubMed: 24140625]
71. a) Hövener JB, Schwaderlapp N, Borowiak R, Lickert T, Duckett SB, Mewis RE, Adams RW, Burns MJ, Highton LAR, Green GGR, Olaru A, Hennig J, von Elverfeldt D. Anal Chem. 2014; 86:1767–1774. [PubMed: 24397559] b) Zeng H, Xu J, McMahon MT, Lohman JAB, van Zijl PCM. J Magn Reson. 2014; 246:119–121. [PubMed: 25123540] c) Mewis RE, Atkinson KD, Cowley MJ, Duckett SB, Green GGR, Green RA, Highton LAR, Kilgour D, Lloyd LS, Lohman JAB, Williamson DC. Magn Reson Chem. 2014; 52:358–369. [PubMed: 24801201]

Author Manuscript Author Manuscript Author Manuscript Author Manuscript

72. Truong ML, Shi F, He P, Yuan B, Plunkett KN, Coffey AM, Shchepin RV, Barskiy DA, Kovtunov KV, Koptyug IV, Waddell KW, Goodson BM, Chekmenev EY. J Phys Chem B. 201410.1021/jp510825b

73. Shi F, Coffey AM, Waddell KW, Chekmenev EY, Goodson BM. Angew Chem Int Ed. 2014; 53:7495–7498.

74. Cunningham CH, Chen AP, Albers MJ, Kurhanewicz J, Hurd RE, Yen YF, Pauly JM, Nelson SJ, Vigneron DB. J Magn Reson. 2007; 187:357–362. [PubMed: 17562376]

75. a) Larson PEZ, Hu S, Lustig M, Kerr AB, Nelson SJ, Kurhanewicz J, Pauly JM, Vigneron DB. Magn Reson Med. 2011; 65:610–619. [PubMed: 20939089] b) von Morze C, Sukumar S, Reed GD, Larson PEZ, Bok RA, Kurhanewicz J, Vigneron DB. Magn Reson Imaging. 2013; 31:163–170. [PubMed: 22898680] c) Perman WH, Bhattacharya P, Leupold J, Lin AP, Harris KC, Norton VA, Hoevener JB, Ross BD. Magn Reson Imaging. 2011; 28:459–465. [PubMed: 20171034]

76. Sarracanie M, Armstrong BD, Stockmann J, Rosen MS. Magn Reson Med. 2014; 71:735–745. [PubMed: 23475813]

77. a) Lupo JM, Chen AP, Zierhut ML, Bok RA, Cunningham CH, Kurhanewicz J, Vigneron DB, Nelson SJ. Magn Reson Imaging. 2010; 28:153–162. [PubMed: 19695815] b) Albers MJ, Bok R, Chen AP, Cunningham CH, Zierhut ML, Zhang VY, Kohler SJ, Tropp J, Hurd RE, Yen YF, Nelson SJ, Vigneron DB, Kurhanewicz J. Cancer Res. 2008; 68:8607–8615. [PubMed: 18922937]

78. Mazzanti ML, Walvick RP, Zhou X, Sun YP, Shah N, Mansour J, Gereige J, Albert MS. PLoS One. 2011; 6:7.

79. Rao, M.; Stewart, N.; Norquay, G.; Wild, J. Proc. Intl. Soc. Mag. Reson. Med; Milan, Italy. 2014. p. 3532Rao, M.; Stewart, N.; Norquay, G.; Wild, J. COST Meeting, Vol. Working group; Zurich, Switzerland. 2014.

80. Gallagher FA, Bohndiek SE, Kettunen MI, Lewis DY, Soloviev D, Brindle KM. J Nucl Med. 2011; 52:1333–1336. [PubMed: 21849405]

Author Manuscript Author Manuscript Author Manuscript Author Manuscript

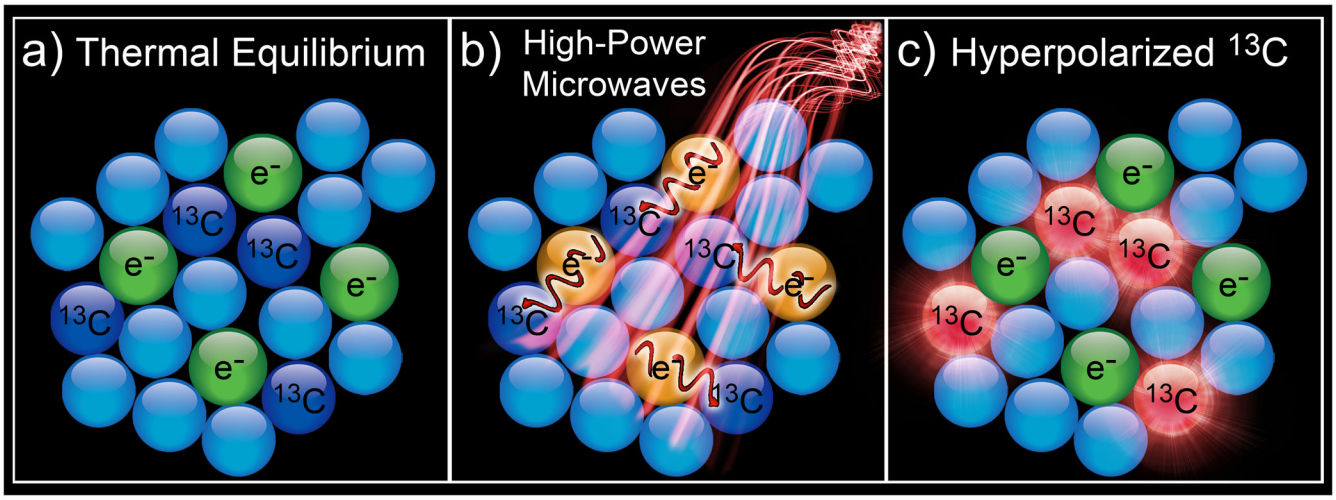

Figure 1.

The process of Dynamic Nuclear Polarization (DNP) using high-power microwave irradiation of electron spins at low temperatures (few Kelvin) and high magnetic field (several Tesla). (a) Glass matrix containing ^{13}C-labeled metabolite and radicals with unpaired electron is formed inside the high-field DNP magnet at low temperature. (b) High-power microwave irradiation at the electron resonance frequency enables ^{13}C hyperpolarization via polarization transfer from free electrons. (iii) A long-lived ^{13}C hyperpolarized state is prepared.

Author Manuscript Author Manuscript Author Manuscript Author Manuscript

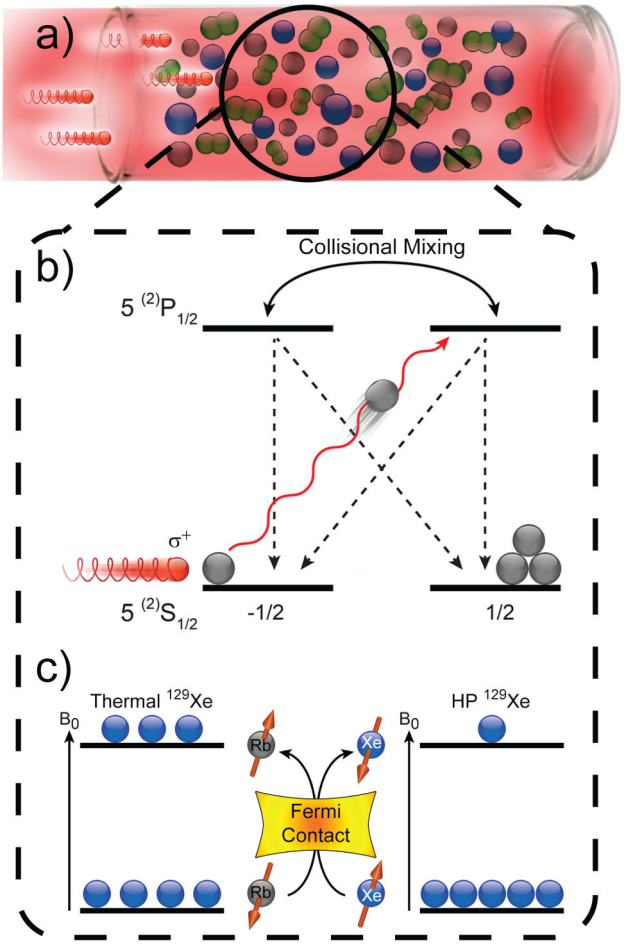

Figure 2.

Spin-Exchange Optical Pumping.[9] (a) SEOP requires an optical cell containing a noble gas, buffer gases (e.g. N_2, as shown), and a small quantity of vaporized alkali metal (typically Rb or Cs[47]), irradiated by laser light resonant with an absorption line of the alkali metal (e.g. 794.8 nm for Rb D_1 transition). Collisions with N_2 non-radiatively quench excited Rb states, effectively suppressing deleterious Rb fluorescence that can depolarize other Rb spins.[48] The first step of SEOP involves the absorption of photons of the same circular polarization, which conserves angular momentum by selectively depleting population from one of two Rb ground electronic (m_J=±1/2) states (neglecting Rb nuclear spin for simplicity). Collisions with other gas-phase species tend to equalize the excited-state populations and the ground states are repopulated at effectively equal rates. However, since only one ground state is depleted by the laser, ground-state population accumulates on the other m_J state, leaving the Rb electronically spin-polarized; a weak magnetic field along the direction of laser propagation (not shown) helps to maintain the electron spin polarization. Gas-phase collisions also allow spin exchange (c) between the polarized Rb electron spins and the noble gas nuclear spins, a process mediated by Fermi-contact hyperfine interactions. Constant laser illumination of the Rb vapor therefore allows the nuclear spin polarization to accumulate over time, thereby generating the hyperpolarized noble gas.

Author Manuscript Author Manuscript Author Manuscript Author Manuscript

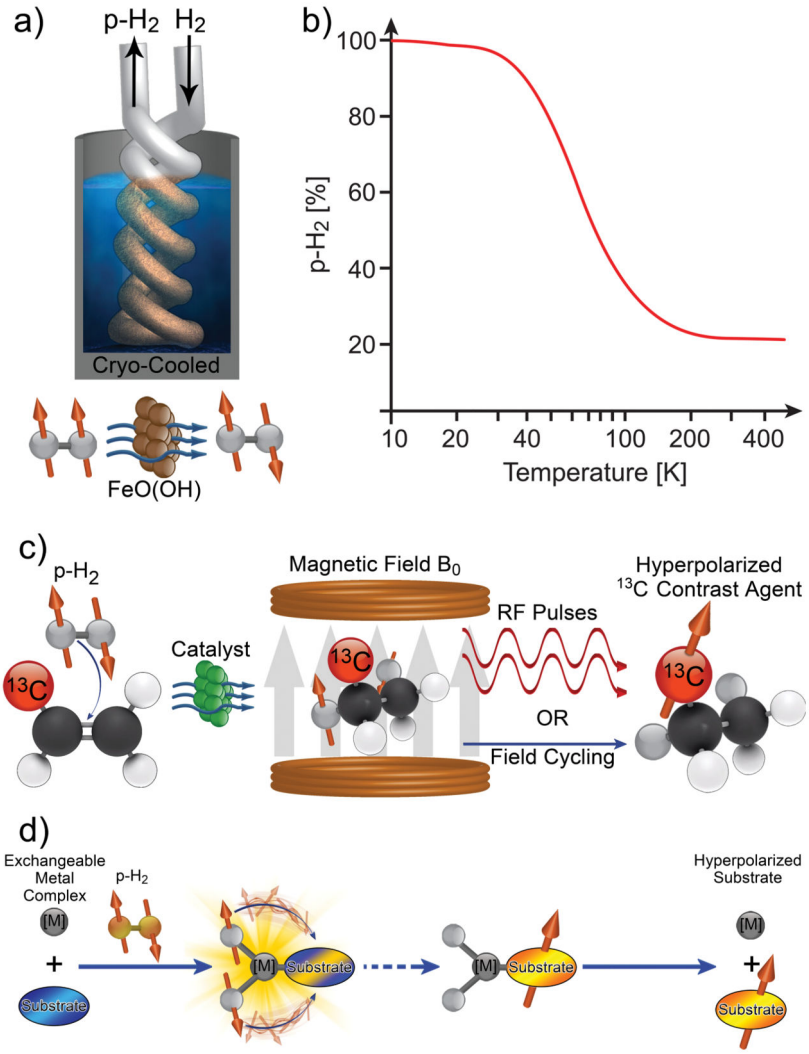

Figure 3.

a–b) Conversion of 'normal' H_2 gas (75% ortho- and 25% para-isomers) into parahydrogen (p-H_2). a) Schematic of a p-H_2 generator, where the entering room-temperature ('normal') H_2 gas is cryo-cooled to ≤77 K and catalytically converted under local equilibrium to a mixture of spin isomers that preferentially favors p-H_2. Because the catalyst is confined to a cryogenically cooled chamber of the polarizer, once the p-H_2 leaves the chamber it is kinetically trapped in the para-state. b) Temperature dependence of the equilibrium p-H_2 percentage. Liquid N_2 temperature (77 K) allows for preparation of 50% p-H_2, whereas temperatures below 20 K enable production of >97% p-H_2 fraction. c) The process of Parahydrogen Induced Polarization (PHIP). The pairwise addition of a p-H_2 molecule to a molecular precursor, which is typically accomplished across a C=C or C≡C bond adjacent to a ^{13}C nucleus using a hetero- or homogeneous catalyst. The resulting chemically 'unlocked' nuclear spin hyperpolarization of the nascent, magnetically inequivalent protons can be used as-is, or transferred to the typically longer-lived (greater T_1) ^{13}C site using either a RF pulse sequence or a field-cycling method. d) The process of Signal

Author Manuscript Author Manuscript Author Manuscript Author Manuscript

Amplification by Reversible Exchange (SABRE). A metal complex [M] enables *p*-H_2 and a substrate to be transiently co-located under conditions of dynamic exchange, resulting in spontaneous polarization transfer[11, 62] from *p*-H_2 to the substrate.

Author Manuscript Author Manuscript Author Manuscript Author Manuscript

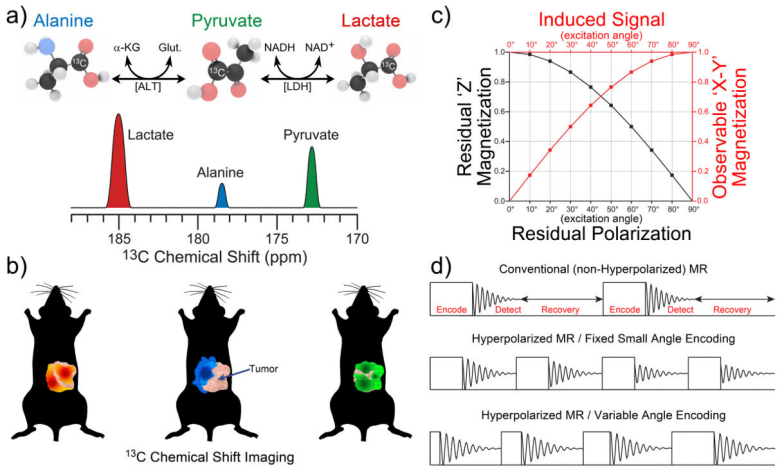

Figure 4.

MR detection concepts of HP contrast agents. a) *In vivo* administration of HP 1-^{13}C-pyruvate leads to its *in vivo* uptake as well as its subsequent metabolism to 1-^{13}C-alanine (using alanine transaminase [ALT]), 1-^{13}C-lactate (using lactate dehydrogenase [LDH]), which can be differentiated using ^{13}C chemical shifts, and b) detected using Chemical Shift Imaging (CSI) to simultaneously produce multiple metabolic maps. Note the red (lactate), blue (alanine) and green (pyruvate) color coding in a) and b). c) Trigonometric dependence of observed (sine) and remaining (cosine) magnetization as a function of RF pulse excitation (or "tipping") angle. d) Fundamental blocks of RF pulse sequences for conventional MR (top); hyperpolarized (HP) MR with fixed small-angle encoding pulses (middle), and HP MR with variable-angle encoding pulses (bottom).

Author Manuscript Author Manuscript Author Manuscript Author Manuscript

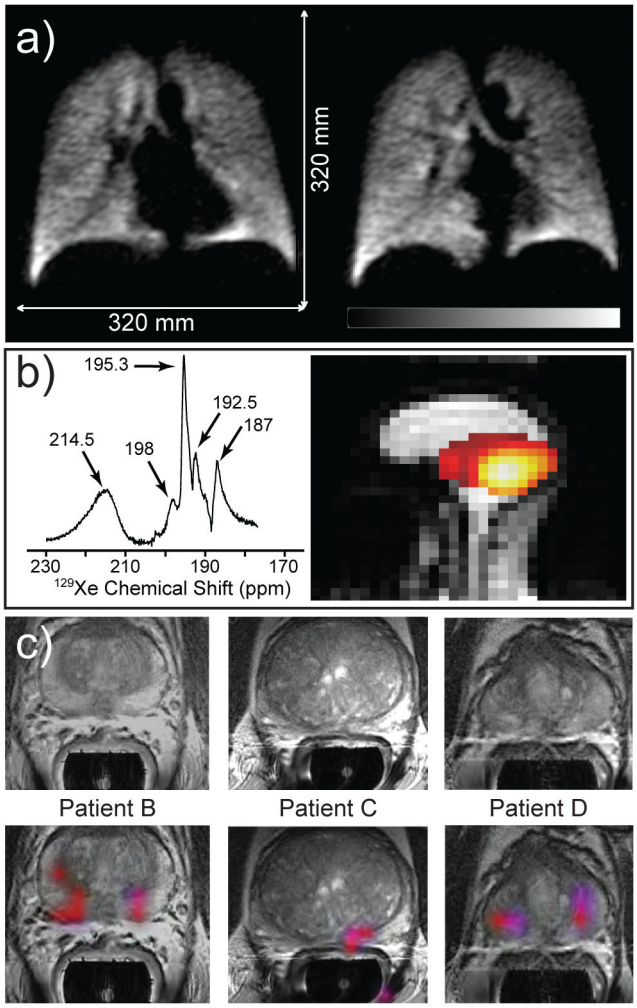

Figure 5.

Examples of biomedical use of hyperpolarized contrast agents in human subjects for pulmonary functional imaging,[5b] spectroscopy and imaging of brain uptake of ^{129}Xe,[79] and molecular imaging of prostate cancer.[27] a) Two slices selected from a 3D ^{129}Xe GRE chest image from a healthy human volunteer following inhalation of HP Xe from an 800-cc Tedlar bag containing a mixture of HP Xe (86%-enriched ^{129}Xe) : 35% N_2, 65 : 35. Subject performed two respiration cycles (total lung capacity to functional residual capacity), inhaled from bag, and then took a small gulp of air (to help push HP Xe out of the trachea); TE/TR, 1.12/11 ms (specific absorption rate-limited); tipping angle, 6°; 80 × 80 × 14; acquisition time, 4.5 s; FOV, 320 × 320 × 196 mm^3; 2 × 2 × 14 mm^3 digital resolution after zero-filling (SNR ~8–15)[5b] b) Left: HP ^{129}Xe spectrum from the brain of a healthy human subject following inhalation of HP Xe from a 1 L Tedlar bag containing Xe : N_2 gas mixture (85 : 15 by volume) (^{129}Xe enrichment: 87%; P_{Xe}~60%). Tentative assignment: 214.5 ppm: red blood cells (RBCs); 198 ppm: blood plasma; 195.3 ppm: grey matter; 192.5 ppm: white matter; 187 ppm: lipid (15 scans; TR=2 s; pulse tipping angle: ~55–65º). Right: sagittal ^{129}Xe MR image (false color) of a healthy human subject overlayed on a corresponding greyscale ^{1}H image following inhalation of HP Xe (same as above, but 100%

Author Manuscript Author Manuscript Author Manuscript Author Manuscript

Xe in bag). ^{129}Xe image shows the signal from the Xe/RBC resonance alone (214.5±0.5 ppm; 2D pulse-acquire; 8X8 matrix of FIDs (zero-filled to 32×32) with 256 points; FOV = 30 cm; slice thickness = 20 cm; pulse tipping angle: ~20º; TR=0.3 s; total ^{129}Xe imaging time: ~20 s). Figures generously provided by Madhwesha Rao, U. Sheffield, UK.[79] c) Representative examples of 3D single-time-point Magnetic Resonance Spectroscopic Imaging (MRSI) data of three prostate cancer subjects after IV injection of HP 1-^{13}C-pyruvate.[27] The axial T_2-weighted images and false-color overlays of hyperpolarized 1-^{13}C-lactate/1-^{13}C-pyruvate ratio are from the three patients labeled as B, C, and D. All three of the patients had biopsy-proven Gleason grade 3 + 3 prostate cancer and received the highest dose of hyperpolarized 1-^{13}C-pyruvate (0.43 ml/kg). Patients B, C, and D had current PSAs of 5.1, 9.8, and 1.9 ng/ml, respectively. The SNR and metabolite ratios in the regions highlighted in color on the image overlays are given in Table 2 of Ref. [27] From S. J. Nelson, et al., Sci. Transl. Med. 2013, 5, 198ra108. Reprinted with permission from AAAS.